forests

MDPI

Article

Integrated Transcriptomic and Metabolomic Analyses Reveal Key Regulatory Pathways Involved in Grafting in *Camellia oleifera*

Yayan Zhu [1,2], Qinmeng Zeng [1], Feng Xiao [2,3], Xueyan Jian [1], Fang Li [1,2], Jiajuan Xu [1,2], Yingying Wei [1], Hui Li [1] and Jie Xu [1,2,*]

[1] Guizhou Academy of Forestry, Guiyang 550005, China; zyynjfu@163.com (Y.Z.); fafuzqm@163.com (Q.Z.); jianxy1966@126.com (X.J.); qq291989555@163.com (F.L.); rrylxjj@163.com (J.X.); ycyy0722@163.com (Y.W.); sanyuan813@163.com (H.L.)
[2] Guizhou Key Laboratory of Forest Cultivation in Plateau Mountain, Guiyang 550025, China; fxiao@gzu.edu.cn
[3] Institute for Forest Resources and Environment of Guizhou, Guizhou University, Guiyang 550025, China
* Correspondence: xuji588@126.com

Abstract

Camellia oleifera is a significant woody oil tree species native solely to China. The bud–seedling grafting technique has been widely applied to this tree due to its significant advantages in improving propagation efficiency and shortening the growth cycle. However, the healing process and its underlying molecular regulatory mechanisms during interspecific heterografting in *Camellia* remain poorly understood. In this study, we established both homografting and heterografting systems using *C. oleifera* bud seedlings as rootstocks, grafted with scions from *C. oleifera*, *C. meiocarpa*, and *C. weiningensis*. We systematically investigated the response patterns and differences in metabolites and gene expression before and after grafting healing through endogenous hormone detection, LC-MS untargeted metabolomics, and transcriptomic sequencing. The results showed that the grafting survival rates between *C. oleifera* and the other species were high (>88%), indicating strong compatibility. Metabolomic analysis revealed that differential metabolites, such as Gibberellin A53, Sophoramine, and Morellin, accumulated significantly with prolonged grafting time, and interspecific grafting combinations exhibited specific highly expressed metabolite profiles. We integrated multi-dimensional data comprising hormone levels, differential metabolites, and DEGs. A "hormone-gene" interaction network was constructed using WGCNA. The analysis revealed that key hub genes, including *CYP73A*, *F3H*, *CHS*, *LHCA1*, and *LHCB5*, were significantly correlated with flavonoid biosynthesis and elevated iPR content. We hypothesize that these genes enhance graft healing capacity by regulating secondary metabolism and hormone signaling pathways. The identified candidate genes, phytohormones, and metabolites provide potential molecular markers and regulatory targets for evaluating graft compatibility, selecting suitable rootstock–scion combinations, and optimizing grafting and propagation practices in *C. oleifera*, providing a crucial theoretical basis for superior cultivar breeding and the investigation of graft compatibility mechanisms.

Keywords: *Camellia oleifera*; transcriptomic; heterograft; endogenous hormones

Check for updates

Academic Editor: John E. Carlson

Received: 2 June 2026
Revised: 17 July 2026
Accepted: 24 July 2026
Published: 28 July 2026

Copyright: © 2026 by the authors. Licensee MDPI, Basel, Switzerland. This article is an open access article distributed under the terms and conditions of the Creative Commons Attribution (CC BY) license.

1. Introduction

Grafting is the process of tightly connecting an organ such as a bud or branch from one plant onto another plant with a root system. Superior grafted plants can combine the respective advantages of the scion and rootstock, such as improvements in yield, quality, and nutrient uptake [1,2]. Successful graft union formation involves a series of steps, including alignment of the vascular cambium, initiation of wound healing responses, and formation of a callus bridge, followed by regeneration of the vascular cambium and subsequent development of secondary xylem and phloem [3]. This is significant for selecting rootstocks with desirable traits, achieving more rational and effective scion–rootstock combinations, and promoting the efficient application of grafting techniques in horticultural crops.

Camellia oleifera belongs to the genus *Camellia* of the family Theaceae and is one of the important woody oil tree species in southern China, characterized by a long cultivation history, wide distribution, large cultivation area, and multiple uses. Tea seed oil is rich in vitamins, sterols, squalene, polyphenols, tea saponins and other bioactive compounds, giving it significant economic and medicinal value [4]. Wild relatives of common *C. oleifera* are valuable genetic resources for tea oil breeding. China possesses abundant tea oil germplasm resources. Major cultivated *Camellia* species with considerable cultivation area and history in China include: *C. oleifera*, *C. meiocarpa*, *C. vietnamensis* and *C. chekiangoleosa*. Guizhou Province is one of the main tea oil production areas in China, ranking fifth nationwide in cultivation area. The primary species cultivated in the province are *C. oleifera*, *C. meiocarpa* and *C. weiningensis*. Due to its large sowing area and wide adaptability, *C. oleifera* is commonly used as rootstock for the rapid propagation of special tea oil cultivars through grafting. Because *C. meiocarpa* and *C. weiningensis* have small seeds and thin seedlings, *C. oleifera* seeds are typically used as rootstock in production.

Budding rootstock grafting is the primary method for asexual propagation of *C. oleifera*, and grafting compatibility is a key factor affecting grafting survival rate. The growth of *C. oleifera* seedlings is influenced by interactions between the scion and rootstock. Homografting exhibits a high survival rate of up to 94%. When ‘Changlin 3’ is used as the rootstock, root system development is affected by the scion and is weaker compared to homografting [5]. Our research group measured the height growth of *C. oleifera*, *C. meiocarpa* and *C. weiningensis* grafts seven months after grafting, which were 25.6 cm, 12.5 cm and 5.3 cm, respectively. Significant differences in height growth were observed, and the sprouting rate and survival rate of *C. weiningensis* were significantly lower than those of *C. oleifera* and *C. meiocarpa*. Currently, it remains unclear whether such heterografting affects graft union healing rate or causes changes in metabolites. This study uses endogenous plant hormone analysis, untargeted metabolomics and transcriptome profiling to identify dynamic differences in hormones, metabolites and gene expression during homografting and heterografting healing processes in *C. oleifera*. The findings lay the foundation for identifying grafting compatibility and molecular breeding of superior varieties.

2. Materials and Methods

2.1. Materials

Our research group previously collected high-quality germplasm resources of different *Camellia* species through field resource surveys. After fruit maturity and harvest, large, plump seeds were selected and stored in sand. In mid-to-late May, when the embryonic shoots reached approximately 3 cm in length, they were used as rootstocks, and semi-lignified scions were collected for grafting. Based on preliminary bud grafting experiments, grafting was performed between *C. oleifera* and *C. meiocarpa* or *C. weiningensis* (grafting combinations: *C. oleifera*/*C. oleifera*, *C. meiocarpa*/*C. oleifera*, *and C. weiningensis*/*C. oleifera*).

The above grafted *Camellia* seedlings are cultivated at the Guizhou Camellia Engineering Technology Research Center (Nanming District, Guiyang City, Guizhou Province, China). Graft union samples were collected from the plants before grafting and at 7, 14, 21, and 28 days post-grafting, with 30 plants sampled per combination. Each treatment was replicated biologically three times. Some combinations began to form callus bridges at 14 days after grafting, and complete union formation was observed by 28 days. The samples were promptly enclosed in aluminum foil, flash-frozen in liquid nitrogen for no less than 30 min, and subsequently stored in an ultra-low temperature freezer set at −80 °C.

2.2. Targeted Determination and Analysis of Endogenous Hormones

The above-mentioned sample tissues were extracted into centrifuge tubes, and the determination was performed using LC-ESI-MS/MS (UHPLC-Qtrap), following the procedures described by Zhu et al. (2025) [6].

2.3. LC-MS Metabolite Profiling and Analysis

Approximately 100 mg of the aforementioned sample was weighed into a centrifuge tube and extracted with a methanol–water solution (4:1, v/v). Samples underwent cryogenic grinding and low-temperature sonication. Following incubation at −20 °C for 30 min, samples were centrifuged (13,000× g, 15 min, 4 °C), and the supernatants were collected. Quality control (QC) samples were prepared by pooling equal volumes of all samples. Metabolite profiling was performed using a UHPLC–Q Exactive system. The raw data were processed for peak picking, alignment, and normalization. Metabolites were annotated by matching both MS and MS/MS spectral information against the Majorbio Plant Metabolome Database (MJDBPM). The matching procedure considered precursor-ion mass, isotopic patterns, and MS/MS fragmentation spectra. Because authentic standards were not used to confirm all metabolites, the identified compounds were regarded as putatively annotated metabolites rather than definitively confirmed compounds. The identification of significantly altered metabolites was performed using OPLS-DA. Candidates were considered significant if they met the criteria of VIP > 1, $p < 0.05$, and $|\text{fold change}| > 1$.

2.4. RNA Library Construction and Transcriptome Analysis

Total RNA was extracted from the samples using Trizol. RNA integrity was assessed by gel electrophoresis, and concentration and purity were measured using a Nanodrop2000. The criteria for RNA quality were: RNA concentration ≥ 30 ng/μL, RIN > 6.5, and OD260/280 ratio between 1.8 and 2.2. Eukaryotic mRNA has a poly-A tail at the 3′ end, which allows for binding to Oligo(dT)-coated magnetic beads through A-T base pairing. After adding fragmentation buffer to randomly break the mRNA into approximately 300 bp fragments, reverse transcription was performed using random primers to synthesize the first-strand cDNA. Following second-strand synthesis, the double-stranded cDNA was end-repaired and A-tailed to facilitate adapter ligation. After purification and size selection, the constructs were enriched via PCR. A final purification step was performed to obtain the sequencing libraries. Quality control of the libraries was performed before sequencing on the Illumina NovaSeq 6000 platform in paired-end mode. Quality control of raw data was conducted using fastp v 0.23.4 software [7]. Clean data were aligned to the reference genome [8] using HiSat2 v2.2.2 with default values [9], and gene expression levels were quantified using RSEM v1.3.3 [10]. Differential expression analysis was performed using DESeq2 v1.50.2 [11] with thresholds set at $|\log_2 FC| > 1$ and p-adjust < 0.05 for identifying differential expression genes (DEGs). Functional enrichment analyses for GO and KEGG pathways were carried out using the clusterProfiler v4.8.1 R package [12]. Using the WGCNA R package (v1.72.1) [13], co-expression modules were generated from DEGs and genes with FPKM > 5 in at least one sample. The pickSoftThreshold function was employed

to identify the optimal soft-thresholding power based on scale-free topology criteria, selecting the value provided by sft$powerEstimate. Subsequent network construction used a minModuleSize of 30 and a MEDissThres of 0.25.

2.5. RT-qPCR

RT-qPCR validation of six genes was conducted using *GAPDH* as the endogenous control to confirm transcriptome reliability. Following primer design via Primer 5.0 (Table S1), reactions were run with an initial denaturation at 95 °C for 30 s and 40 cycles of 94 °C for 5 s and 60 °C for 15 s. Expression data were analyzed using the $2^{-\Delta\Delta Ct}$ formula [14].

2.6. Data Analysis

All statistical analyses were performed in R v4.5.2. Data were subjected to one-way analysis of variance (ANOVA) using the 'aov' function, followed by Fisher's least significant difference (LSD) test for post hoc multiple comparisons. Correlation analysis was performed using the 'ggstatsplot' v0.13 package, and principal component analysis (PCA) was conducted using the 'factoextra' v1.0.7 package.

3. Results

3.1. Analysis of Endogenous Hormone Contents

Analysis of plant endogenous hormones in different grafting combinations revealed that ABA content increased immediately after grafting and then gradually decreased over time (Figure 1a). GA_1 content in *C. weiningensis* continuously increased with grafting time (Figure 1b). JA content was relatively high in all three species before grafting (Figure 1c). SA and GA_7 levels in *C. meiocarpa* were significantly higher than those in *C. oleifera* and *C. weiningensis* prior to grafting (Figure 1d,e). cZR content was relatively high in all three species at 14 days after grafting (Figure 1f). IAA content in *C. meiocarpa* was relatively high at 14 days after grafting (Figure 1g). iP content in *C. meiocarpa* was relatively high at 7 days after grafting (Figure 1h). iPA content in *C. meiocarpa* was also relatively high at 7 days after grafting (Figure 1i). iPR content significantly increased after grafting in all three grafted combinations compared to pre-grafting levels (Figure 1j). OPDA, tZ, and tZR contents in *C. weiningensis* showed a trend of first increasing and then decreasing after grafting (Figure 1k–m). Correlation analysis revealed a significant positive correlation between IAA and iPA (r = 0.89) (Figure S1a). PCA indicated that the spatial distances among different grafting combinations were relatively close at 7 and 14 days after grafting (Figure S1b).

3.2. Analysis of Untargeted Metabolomics

Metabolites from different grafting combinations were analyzed using untargeted liquid chromatography-tandem mass spectrometry (LC-MS/MS). Based on KEGG Compound secondary classification annotations, compounds such as amino acids, carboxylic acids, and monosaccharides were identified (Figure 2a). According to HMDB classification annotations, lipids and lipid-like molecules (591), phenylpropanoids and polyketides (305), organic acids and derivatives (213), and organic oxygen compounds (200) were annotated (Figure 2b). PCA of the metabolite profiles showed that PC1 along the *X*-axis accounted for 31.5% and PC2 along the *Y*-axis accounted for 19.1%, with a high cumulative contribution rate (Figure 2c), and good reproducibility was observed among replicates of the same combination. Hierarchical clustering analysis of all metabolites (Table S2) revealed that metabolites in cluster 1 exhibited an increasing trend over time after grafting across different species (Figure 2d_1). Metabolites in cluster 2 were relatively more abundant in *C. meiocarpa* (Figure 2d_2). Metabolites in cluster 3 were relatively more abundant in

C. weiningensis (Figure 2d_3). Metabolites in cluster 6 were relatively more abundant in *C. oleifera* (Figure 2d_6).

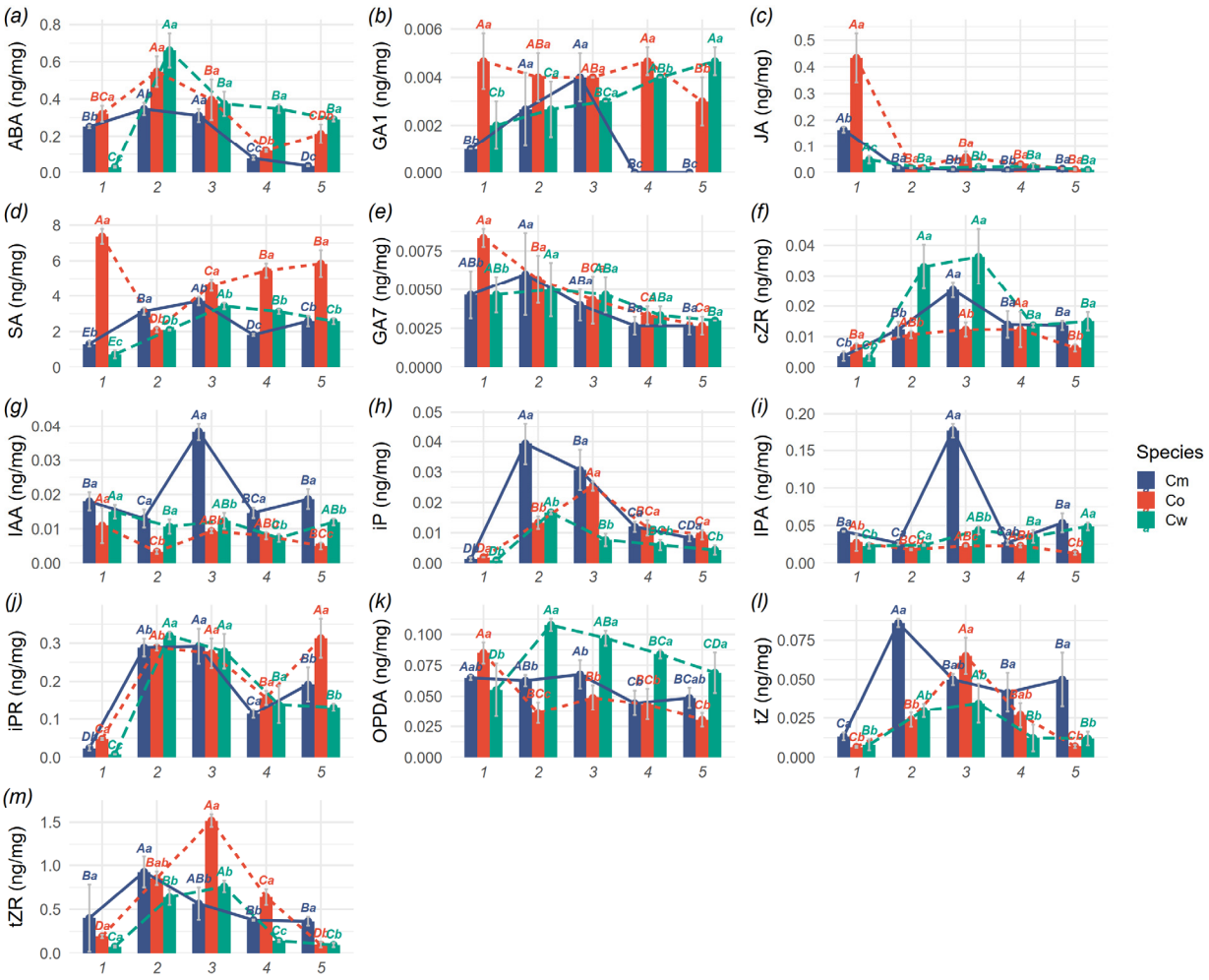


Figure 1. Changes in endogenous hormone levels in different Camellia species before and after grafting. (**a**): ABA; (**b**): GA1; (**c**): JA; (**d**): SA; (**e**): GA7; (**f**): cZR; (**g**): IAA; (**h**): iP; (**i**): IPA; (**j**): iPR; (**k**): OPDA; (**l**): tZ; (**m**): tZR; Note: Different capital letters indicate significant differences in the same species at different time points; different lowercase letters indicate significant differences among species at the same time point. Multiple comparisons were performed using the LSD method. Co: *C. oleifera*, Cm: *C. meiocarpa*, Cw: *C.weiningensis*. 1, 2, 3, 4, 5 represent: before grafting, 7 days, 14 days, 21 days, and 28 days after grafting, respectively.

3.3. Transcriptome Assembly, Annotation, and DEG Identification

Sequencing was completed for 45 samples, yielding a total of 309.96 Gb of clean data, with each sample having more than 5.88 Gb of clean data and a Q30 base percentage exceeding 95.51%. Clean reads from all samples were mapped to the reference genome, yielding alignment rates between 74.93% and 79.41%. Correlation analysis among samples (Figure 3a) and PCA (Figure 3b) revealed high correlation between replicates within the same group and close proximity among samples within the same group, indicating good reproducibility.

DEG identification and analysis (Figure 4a and Table S3) showed that compared to Co1, Cm1 had 1042 upregulated genes and 1284 downregulated genes; compared to Cw1, Cm1 had 2850 upregulated genes and 3259 downregulated genes. Cluster analysis of all DEGs (Figure 4b and Table S4) identified that cluster 7 exhibited an increasing trend after grafting across different species, with this trend continuing to increase over time. GO

enrichment analysis of the gene set in cluster 7 revealed enriched biological process (BP) terms such as mitotic cell cycle (GO:0000278), male meiotic nuclear division (GO:0007140), and microtubule-based movement (GO:0007018). KEGG enrichment analysis indicated pathways such as circadian rhythm—plant (ko04712)—were enriched. In cluster 8, *C. weiningensis* showed higher expression levels, with enriched pathways including MAPK signaling pathway—plant (ko04016), stilbenoid, diarylheptanoid, and gingerol biosynthesis (ko00945), phenylpropanoid biosynthesis (ko00940), zeatin biosynthesis (ko00908), sulfur metabolism (ko00920), and necroptosis (ko04217). Cluster 9 exhibited an increasing trend after grafting, followed by a gradual decline over time, with enriched pathways such as photosynthesis protein (ko00194) and flavonoid biosynthesis (ko00941) identified through KEGG enrichment analysis. Genes in cluster 10 were highly expressed in *C. oleifera*, with GO enrichment analysis revealing enriched BP terms such as flavonoid biosynthetic process (GO:0009813) and flavonoid metabolic process (GO:0009812).

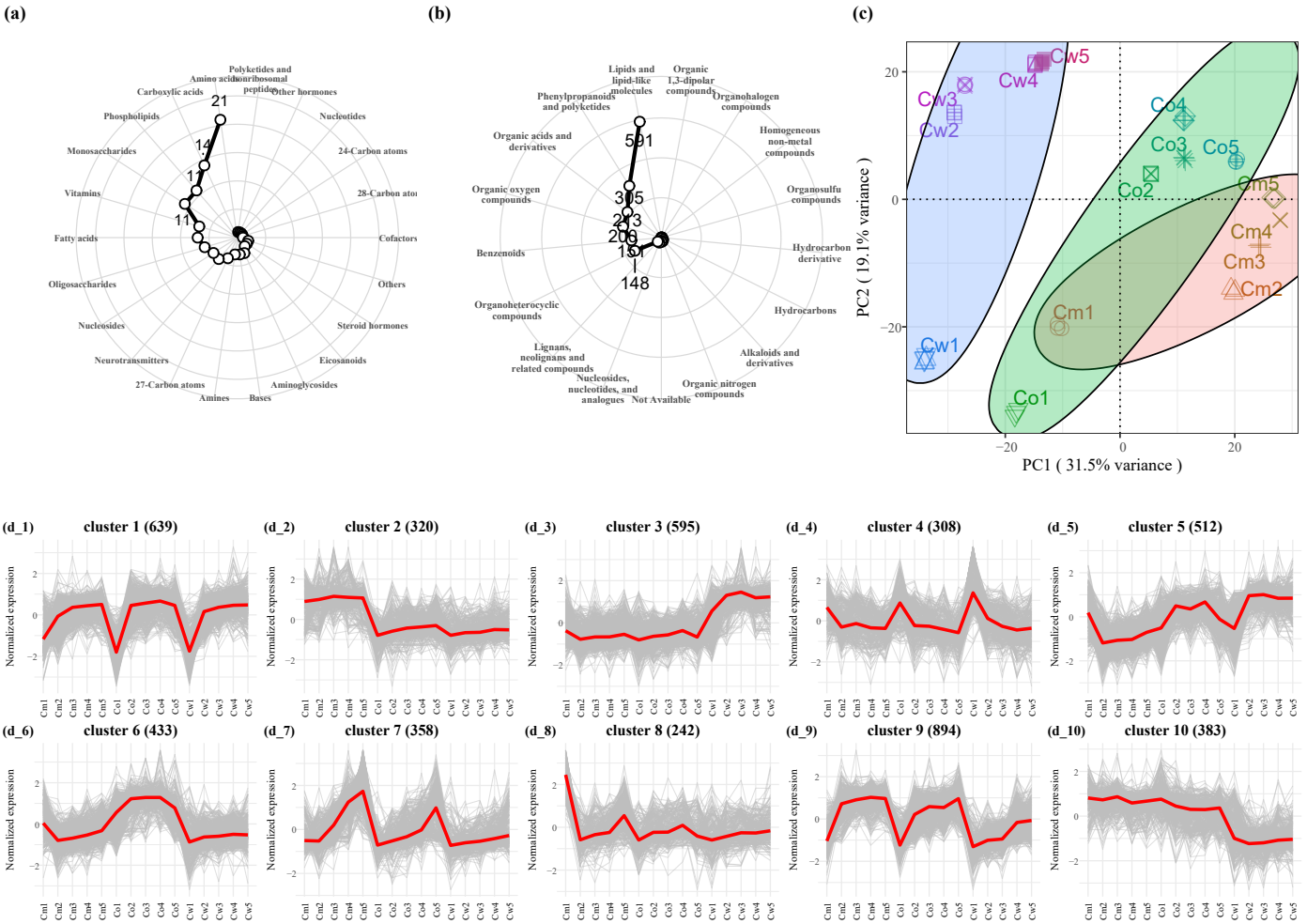


Figure 2. Trend changes in non-targeted metabolites before and after grafting in different Camellia species. (**a**): Annotation of KEGG Compound secondary classifications; (**b**): classification of compounds based on HMDB; (**c**): principal component analysis (PCA); (**d_1–d_10**): cluster clustering submodule; Note: The number of labeled compounds in a exceeds 10; the number of labeled compounds in b exceeds 100; different background colors in C represent different groups; the clustering method used in d1–d10 is mfuzz, with cluster number set to 10. The red line represents the average trend, and each gray line represents a metabolite. 1, 2, 3, 4, and 5 represent: before grafting, 7 days, 14 days, 21 days, and 28 days after grafting, respectively. Co: *C. oleifera*; Cm: *C. meiocarpa*; Cw: *C. weiningensis*.

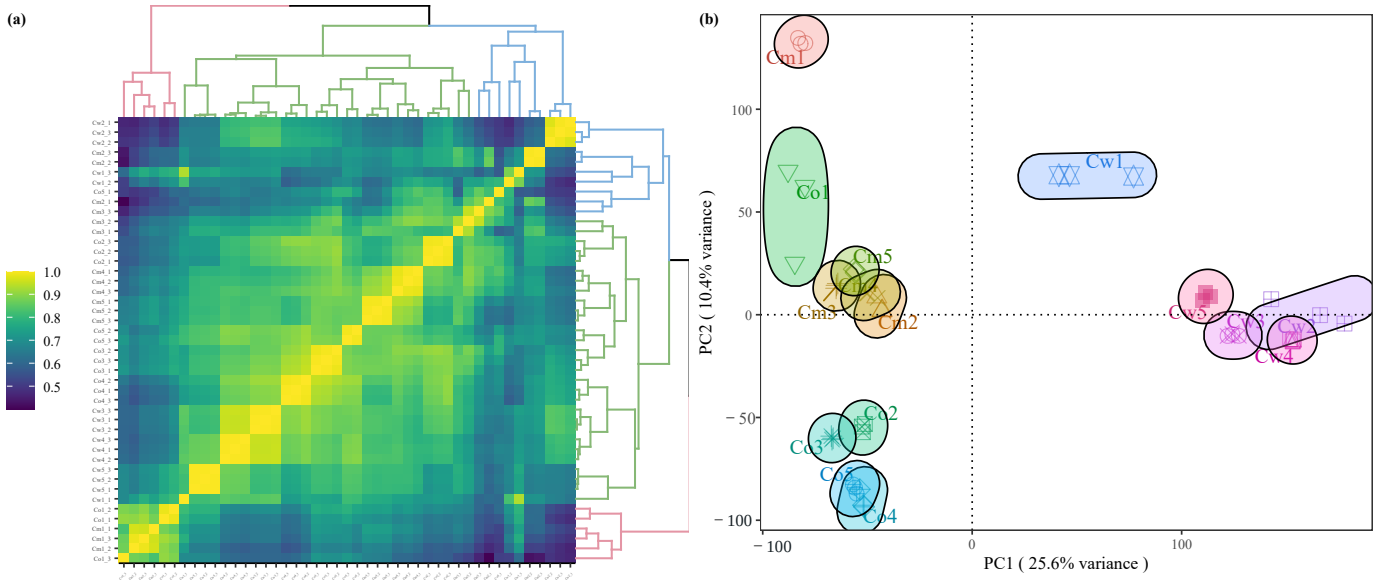


Figure 3. Transcriptome Correlation and Principal Component Analysis. (**a**): Correlation analysis between samples; (**b**): PCA between samples.

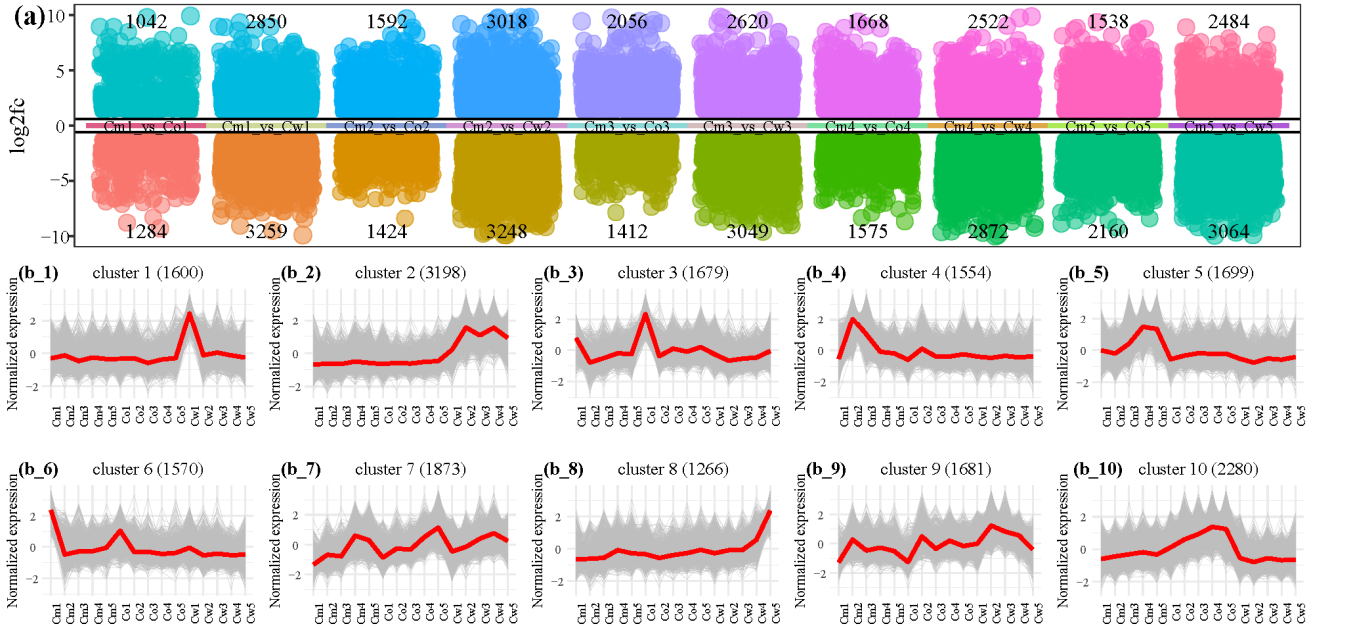


Figure 4. Changes in transcriptional expression trends before and after grafting among different C. oleifera varieties. (**a**): Number of differentially expressed genes between different combinations; (**b_1–b_10**): Cluster clustering submodule. Note: Clustering in panels (**b**) was performed using the mfuzz method with the number of clusters set to 20. The red line represents the average trend, and each gray line represents an individual gene. Time points 1, 2, 3, 4, and 5 represent before grafting, and 7, 14, 21, and 28 days after grafting, respectively.

3.4. WGCNA Analysis

WGCNA analysis indicated that a total of 22 co-expression gene modules associated with traits could be identified (Figure 5a and Table S5). The yellowgreen module (58 genes) showed a significant negative correlation with SA ($r = -0.63$, $p = 4.4 \times 10^{-6}$), with lower expression in *C. oleifera* and higher expression in heterografting combinations (Figure S2a), possibly due to the effects of heterografting. Key hub genes identified within the yellowgreen module include *SART1*, *SPS*, and *RPS30* (Figure 5b).

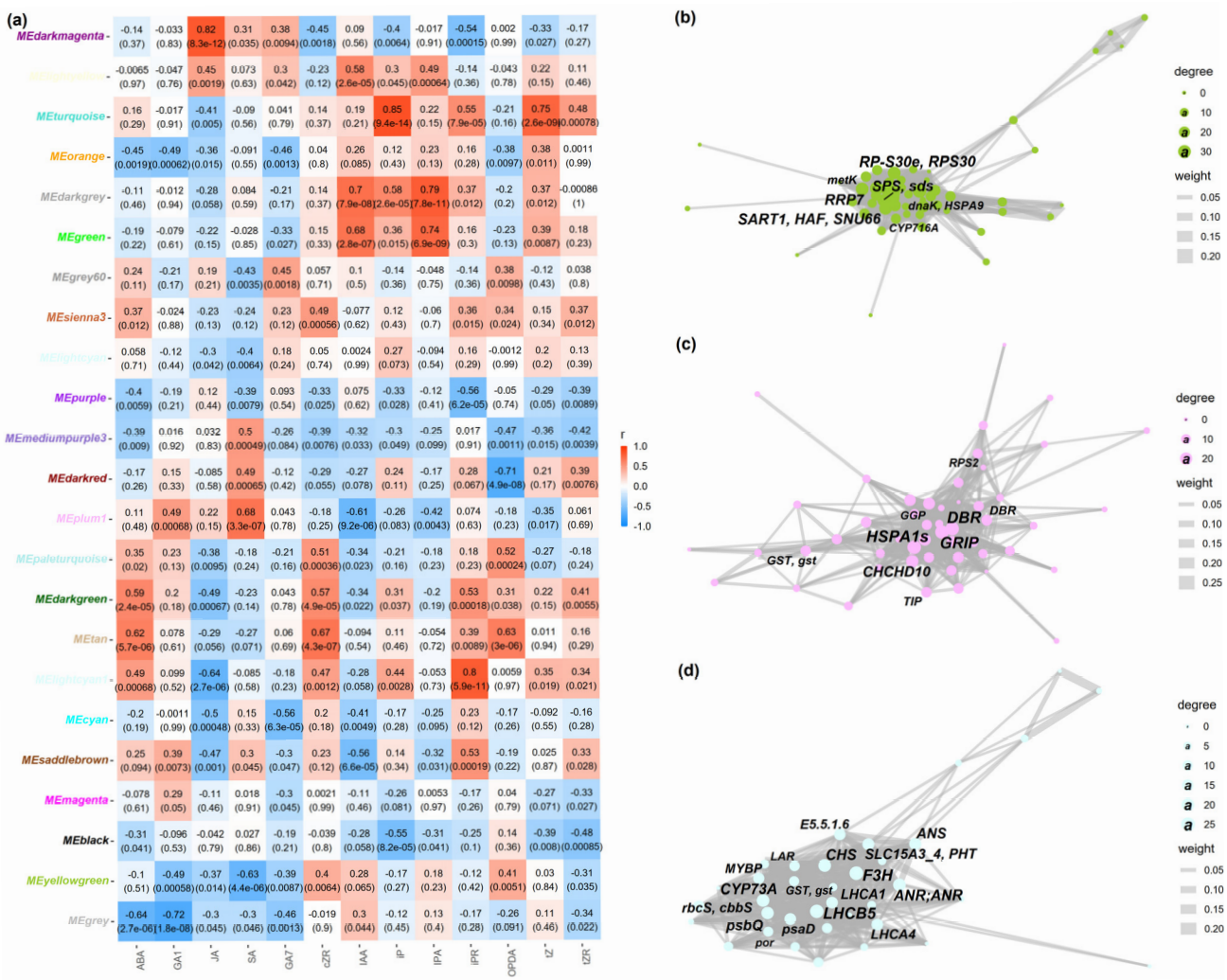


Figure 5. WGCNA Analysis and network visualization (**a**): WGCNA Analysis; (**b**): Network visualization of the yellowgreen module; (**c**): Network visualization of the plum1 module; (**d**): Network visualization of the lightcyan1 module.

The plum1 module (53 genes) exhibited a significant positive correlation with SA (r = 0.68, $p = 3.3 \times 10^{-7}$), showing higher expression in *C. oleifera* and lower expression in heterografting combinations (Figure S2b), which may be related to graft compatibility. GO enrichment analysis revealed terms such as response to toxic substance (GO:0009636), glutathione binding (GO:0043295), 2-alkenal reductase [NAD(P)+] activity (GO:0032440), oxidoreductase activity acting on the CH-CH group of donors, NAD or NADP as acceptor (GO:0016628), and glutathione transferase activity (GO:0004364). KEGG enrichment analysis highlighted pathways including metabolism of xenobiotics by cytochrome P450 (ko00980) and glutathione metabolism (ko00480). Hub genes identified in the plum1 module include *GRIP*, *DBR*, *GST*, and *HSPA1* (Figure 5c).

The lightcyan1 module (36 genes) showed a significant positive correlation with iPR (r = 0.8, $p = 5.9 \times 10^{-11}$), with expression levels increasing post-grafting across all three *Camellia* species (Figure S2c), indicating a potential role in healing after grafting. GO enrichment analysis revealed terms related to photosynthesis, light reaction (GO:0019684), and flavonoid biosynthetic process (GO:0009813). KEGG enrichment analysis identified pathways such as photosynthesis proteins [BR:ko00194] (ko00194) and flavonoid biosynthesis (ko00941). Hub genes identified in the lightcyan1 module include *CYP73A*, *F3H*, *CHS*, *LHCA1* and *LHCB5* (Figure 5d).

3.5. RT-qPCR Validation

To validate the reliability of the RNA-seq data, six grafting-related genes were selected from the transcriptome dataset for real-time quantitative PCR (RT-qPCR) analysis. The expression patterns of the six selected genes showed strong concordance between the RNA-seq and RT-qPCR datasets, confirming the high reliability of the transcriptome sequencing results (Figure S1).

4. Discussion

C. oleifera is one of the most important woody oil plants in China [6]. Oleic acid constitutes approximately 80% of its seed oil [15]. *C. meiocarpa*, second only to *C. oleifera* in terms of cultivation area and annual yield, is characterized by high and stable fruiting, thin fruit peel, high seed extraction rate, high oil content, strong stress resistance, and adaptability. It is an important edible woody oil plant with significant ecological and economic value [16]. *C. weiningensis*, a wild oil tea resource primarily distributed in Weining County, Guizhou Province, southwestern China [17], grows at altitudes between 1600 m and 2700 m. Known for its drought and disease resistance, early maturation with spring flowers and autumn fruits, and thin fruit peels and seed shells, it represents an excellent germplasm for developing the oil tea industry in high-altitude areas of Guizhou. Grafting is the primary method for breeding and improving high-quality, high-yield oil tea varieties [18]. Interspecies graft compatibility significantly influences grafting success, where genetic distance is a critical determinant of survival rates—the greater the genetic distance, the lower the survival rate [19]. Using *C. oleifera* seedlings as rootstocks and grafting them with scions from *C. oleifera*, *C. meiocarpa*, and *C. weiningensis*, the respective survival rates were: *C. oleifera*/*C. oleifera* (95%) > *C. meiocarpa*/*C. oleifera* (93%) > *C. weiningensis*/*C. oleifera* (88%). Seven months post-grafting, the heights of the shoots in different combinations were 25.6 cm, 12.5 cm, and 5.3 cm, respectively, indicating that while *C. oleifera*, *C. meiocarpa* and *C. weiningensis* all exhibit relatively high compatibility when grafted onto *C. oleifera*, there are notable differences in growth performance.

Phenotypic analysis has shown that heterografting inhibits the growth vigor of the grafted junction [20]. The effects brought by heterologous rootstocks become evident within two months [19] and can last for over 20 years [21]. Grafting *P. cembroides* and *P. orizabensis* onto four different pine species (*P. cembroides*, *P. patula*, *P. teocote*, and *P. greggii* var. *australis*) significantly affected the number of apical buds, with graft survival rates ranging from 45.5% to 100% [22]. *Chili pepper* plants of the variety "Adige" grafted onto drought-tolerant chili A25 (A/A25) showed greater root biomass, better water absorption and retention capabilities, and sustained CO_2 assimilation rates compared to non-grafted (A) and self-grafted (A/A) plants [23]. In grafted *C. oleifera*, scions significantly influenced the root-to-shoot ratio, morphological characteristics of roots larger than 1 mm in diameter, phosphorus accumulation, and phosphorus use efficiency [24]. In compatible and incompatible graft combinations, hormone balance was disrupted, with two limiting key genes—NCED3 (9-cis-epoxycarotenoid dioxygenase 3) and NCED5—identified as crucial factors controlling ABA accumulation [25]. GO and KEGG enrichment analyses revealed extensive metabolic, physiological, and hormonal responses during the healing process of heterografted seedlings [26]. Plant hormone content measurements found that ABA levels increased after grafting but decreased over time (Figure 1a), with IPR significantly correlated with ABA content (Figure 1i). The iPR content in all three *Camellia* species post-grafting was significantly higher than pre-grafting, indicating an association with injury stress at the graft site. IAA content in *C. meiocarpa* was relatively high 14 days post-grafting (Figure 1g). iP and iPA contents in *C. meiocarpa* were relatively high 7 days post-grafting (Figure 1h,i), with IAA and IPA showing a significant correlation (r = 0.89), potentially

related to intrinsic characteristics of *C. meiocarpa*. Differential metabolites exhibited varying growth trends during post-graft development [27]. LC-MS/MS measurements on different grafting combinations showed good reproducibility among the same combinations. Cluster analysis of all metabolites revealed that cluster 2 had relatively higher contents in *C. meiocarpa* (Figure 2d_2), including P-Coumaroylputrescine, Trioxsalen, Momorcharaside B, Gravolenic acid, Ganoderic acid S, etc. Cluster 3 had relatively higher contents in *C. weiningensis* (Figure 2d_3), including Typhaneoside, Myricetin, Dalfopristin, Bellidifolin, etc. Cluster 6 had relatively higher contents in *C. oleifera* (Figure 2d_6), including Eriodictyol, Coumaroyl quinic acid, Phloretin, Cordeauxione, Acevaltrate, Roquefortine D, etc., likely due to species specificity. Metabolites in cluster 1 showed an increasing trend over time across different species post-grafting (Figure 2d_1), including Gibberellin A53, Sophoramine, Morellin, etc. High-throughput transcriptome sequencing facilitated rapid identification of gene expression differences among different species and tissues. Clustering of differentially expressed genes revealed that cluster 7 showed an increasing trend post-grafting and continued to increase over time. GO enrichment analysis of the gene set in cluster 7 identified enriched biological process terms such as mitotic cell cycle (GO:0000278), male meiotic nuclear division (GO:0007140), and microtubule-based movement (GO:0007018). KEGG enrichment analysis highlighted pathways including Circadian rhythm—plant (ko04712).

WGCNA analysis revealed a total of 22 co-expression gene modules associated with traits (Figure 5a). The yellowgreen module (58 genes) showed a significant negative correlation with SA (r = -0.63, $p = 4.4 \times 10^{-6}$), with lower expression in *C.oleifera* and higher expression in heterografting combinations, possibly induced by heterografting. The plum1 module (53 genes) exhibited a significant positive correlation with SA (r = 0.68, $p = 3.3 \times 10^{-7}$), with higher expression in *C. oleifera* and lower expression in heterografting combinations, suggesting a potential link to grafting compatibility. Hub genes identified within the plum1 module include *GRIP*, *DBR*, *GST*, and *HSPA1s*. The lightcyan1 module (36 genes) was significantly positively correlated with iPR (r = 0.8, $p = 5.9 \times 10^{-11}$), and its expression increased in all three *Camellia* species after grafting compared to pre-grafting levels, indicating an association with post-grafting healing. GO enrichment analysis revealed terms related to photosynthesis, light reaction (GO:0019684) and flavonoid biosynthetic process (GO:0009813). KEGG enrichment analysis indicated enrichment in pathways such as photosynthesis proteins [BR:ko00194] (ko00194) and flavonoid biosynthesis (ko00941). Hub genes identified in the lightcyan1 module include *CYP73A*, *F3H*, *CHS*, *LHCA1* and *LHCB5*, suggesting that these genes may be involved in increased flavonoid and iPR levels, thereby enhancing graft healing capacity. *CHS* and *F3H*, which encode key enzymes in flavonoid biosynthesis, have been reported to exhibit altered expression in grafted plants [28], suggesting that flavonoid metabolism may participate in wound responses and graft-union formation. *CYP73A*, which encodes cinnamate 4-hydroxylase, may contribute to graft-union development by directing metabolic flux toward phenylpropanoid-derived compounds involved in wound defense, flavonoid accumulation, and cell-wall lignification [29]. The differential expression of *LHCA1* and *LHCB5* may reflect changes in photosynthetic activity and energy supply during graft establishment. Because graft-union formation requires substantial carbon and energy investment, maintenance of photosynthetic capacity may indirectly support tissue regeneration. Taken together, these results indicate that the lightcyan1 module may represent a coordinated transcriptional response linking cytokinin dynamics, flavonoid metabolism, photosynthetic adjustment, and tissue regeneration during graft establishment. The simultaneous association of this module with iPR accumulation and the enrichment of photosynthesis- and flavonoid-related genes suggests that hormonal signaling, antioxidant metabolism, and energy supply may act co-

operatively to support wound repair and vascular reconnection. Nevertheless, the WGCNA results are based on co-expression and trait correlations and do not establish direct regulatory relationships. Therefore, *F3H*, *CHS*, *LHCA1* and *LHCB5* should be regarded as candidate genes associated with graft healing, and their specific functions require further validation through gene-expression manipulation, hormone or metabolite treatments, and histological analyses of graft-union development.

5. Conclusions

Using large-seeded *C. oleifera* as rootstocks for bud-grafting on seedling rootstocks is the primary propagation method for *C. oleifera* production in our province. During the graft healing period, the interaction between rootstock and scion not only exhibits distinct histological changes but also involves complex physiological, biochemical, and molecular regulatory mechanisms. In this study, we explored the healing mechanisms of both homografting and heterografting among *C. oleifera*, *C. meiocarpa* and *C. weiningensis* by measuring endogenous hormone levels, transcriptome and metabolome profiles. The results of endogenous hormone measurements showed that ABA content increased after grafting in all three combinations and gradually decreased over time, cZR content was relatively high at 14 days after grafting, and iPR content was significantly higher than pre-grafting levels. In the untargeted metabolomics analysis, the relative abundance of metabolites such as Gibberellin A53, Sophoramine, and Morellin continuously increased with prolonged grafting time. Furthermore, transcriptome analysis revealed that genes including *SART1*, *SPS*, *RPS30*, *CYP73A*, *F3H*, *CHS*, *LHCA1* and *LHCB5* were upregulated or downregulated to varying degrees.

Supplementary Materials: The following supporting information can be downloaded at: https://www.mdpi.com/article/10.3390/f17080880/s1, Table S1. The primer list of qRT-PCR. Table S2. Hierarchical clustering analysis of all metabolites. Table S3. The complete list of DEGs. Table S4. Cluster analysis of all DEGs. Table S5. Gene significance analysis between gene expression and phytohormone contents in WGCNA modules. Figure S1. Correlation analysis and PCA of the endogenous hormone. Figure S2. Expression of eigengenes of selected module. Figure S3. qRT-PCR validation.

Author Contributions: Y.Z.: Writing—original draft, Investigation, Data analysis. Q.Z.: Writing—review and editing, data curation. F.X.: Validation, Software. X.J.: Validation, Investigation. F.L.: Investigation. J.X. (Jiajuan Xu): Formal analysis. Y.W.: Investigation. H.L.: Data curation. J.X. (Jie Xu): Supervision, Resources, Methodology, Funding acquisition, Data curation. All authors have read and agreed to the published version of the manuscript.

Funding: This research was funded by the Science and Technology Department of Guizhou Province (funding number: Qiankehejichu-ZK [2024] zhongdian 091) and the Forestry Bureau of Guizhou Project (grant number:2026-ZM-30, Qianlinkehe [2026]zhongdian 008, Gui [2026]TG5 and Gui [2025]TG02).

Data Availability Statement: The raw sequence data reported in this paper have been deposited in the Genome Sequence Archive in National Genomics Data Center, China National Center for Bioinformation/Beijing Institute of Genomics, Chinese Academy of Sciences (BioProject accession: PRJCA033275) and are publicly accessible at https://ngdc.cncb.ac.cn/gsa (accessed on 5 December 2025).

Conflicts of Interest: The authors declare no conflicts of interest.

References

1. San Bautista, A.; Calatayud, A.; Nebauer, S.G.; Pascual, B.; Maroto, J.V.; López-Galarza, S. Effects of simple and double grafting melon plants on mineral absorption, photosynthesis, biomass and yield. *Sci. Hortic.* **2011**, *130*, 575–580. [CrossRef]
2. Cheng, Y.; Mao, J.; Cao, L.; Wang, H.; Li, S.; Jin, X.; Zhang, X.; Li, Y. Molecular basis of flavonoid accumulation in tea leaves grafted with *Camellia sinensis* var. assamica cv."Yinghong9" as rootstock based on multi-omics analysis. *Sci. Hortic.* **2023**, *321*, 112290. [CrossRef]
3. Rasool, A.; Mansoor, S.; Bhat, K.; Hassan, G.; Baba, T.R.; Alyemeni, M.N.; Alsahli, A.A.; El-Serehy, H.A.; Paray, B.A.; Ahmad, P. Mechanisms underlying graft union formation and rootstock scion interaction in horticultural plants. *Front. Plant Sci.* **2020**, *11*, 590847. [CrossRef] [PubMed]
4. Yang, F.; Zhou, Y.; Du, J.; Wang, K.; Lv, L.; Long, W. Prediction of fruit characteristics of grafted plants of *Camellia oleifera* by deep neural networks. *Plant Methods* **2024**, *20*, 23. [CrossRef] [PubMed]
5. Long Wei, L.W.; Yao XiaoHua, Y.X.; Wang KaiLiang, W.K.; Wang Yi, W.Y. The analysis of the affinity of rootstock and scion in the grafting seedlings of *Camellia oleifera*. *Acta Agric. Univ. Jiangxiensis* **2013**, *35*, 346–351.
6. Zhu, Y.; Xu, J.; Wang, G.; Xiao, F.; Zhang, M.; Zeng, Q.; Xu, J. Integrated Metabolome and Transcriptome Analyses Provides Insights into Ovule Abortion in *Camellia oleifera*. *Plants* **2025**, *14*, 613. [CrossRef] [PubMed]
7. Chen, S.; Zhou, Y.; Chen, Y.; Gu, J. fastp: An ultra-fast all-in-one FASTQ preprocessor. *Bioinformatics* **2018**, *34*, i884–i890. [CrossRef] [PubMed]
8. Lin, P.; Wang, K.; Wang, Y.; Hu, Z.; Yan, C.; Huang, H.; Ma, X.; Cao, Y.; Long, W.; Liu, W. The genome of oil-Camellia and population genomics analysis provide insights into seed oil domestication. *Genome Biol.* **2022**, *23*, 14. [CrossRef] [PubMed]
9. Kim, D.; Langmead, B.; Salzberg, S.L. HISAT: A fast spliced aligner with low memory requirements. *Nat. Methods* **2015**, *12*, 357–360. [CrossRef] [PubMed]
10. Li, B.; Dewey, C.N. RSEM: Accurate transcript quantification from RNA-Seq data with or without a reference genome. *BMC Bioinform.* **2011**, *12*, 323. [CrossRef]
11. Love, M.I.; Huber, W.; Anders, S. Moderated estimation of fold change and dispersion for RNA-seq data with DESeq2. *Genome Biol.* **2014**, *15*, 550. [CrossRef] [PubMed]
12. Wu, T.; Hu, E.; Xu, S.; Chen, M.; Guo, P.; Dai, Z.; Feng, T.; Zhou, L.; Tang, W.; Zhan, L. clusterProfiler 4.0: A universal enrichment tool for interpreting omics data. *Innovation* **2021**, *2*, 100141. [CrossRef] [PubMed]
13. Langfelder, P.; Horvath, S. WGCNA: An R package for weighted correlation network analysis. *BMC Bioinform.* **2008**, *9*, 559. [CrossRef]
14. Livak, K.J.; Schmittgen, T.D. Analysis of relative gene expression data using real-time quantitative PCR and the $2^{-\Delta\Delta CT}$ method. *Methods* **2001**, *25*, 402–408. [CrossRef] [PubMed]
15. Chen, M.; Zhang, Y.; Du, Z.; Kong, X.; Zhu, X. Integrative metabolic and transcriptomic profiling in camellia oleifera and camellia meiocarpa uncover potential mechanisms that govern triacylglycerol degradation during seed desiccation. *Plants* **2023**, *12*, 2591. [CrossRef] [PubMed]
16. Wang, R.; Li, W.; He, Z.; Lyu, H.; Wang, X.; Ye, C.; Xun, C.; Xiao, G.; Zhang, Y.; Zhang, Z. Haplotype-resolved genome assembly of the tetraploid Youcha tree *Camellia meiocarpa* Hu. *Sci. Data* **2025**, *12*, 541. [CrossRef] [PubMed]
17. Xu, H.; Yu, C. Transcriptomic analysis reveals crucial biological pathways associated with cold response in *Camellia weiningensis* in Guizhou Province, China. *Sci. Hortic.* **2022**, *295*, 110883. [CrossRef]
18. Yang, P.; Fu, H.; Sun, P.; Ren, L.; Zheng, Z.; Xu, J.; Lv, L.; Liang, Q.; Yang, D. Shell structure impacts *Camellia oleifera* fruit splitting during dehydration. *Food Bioprod. Process.* **2024**, *148*, 298–308. [CrossRef]
19. Xiao, F.; Zhao, Y.; Wang, X.; Jian, X. The effects of homologous and heterologous grafting on the growth of *Gleditsia sinensis* scions. *Forests* **2023**, *14*, 1777. [CrossRef]
20. Ge, X.; Zhong, Q.; Tan, X.; Wang, J.; Cao, L.; Zhou, Y.; Zou, Y.; Yuan, Y.; Wan, X.; Yan, C. Integrated multi-omics analysis to elucidate the role of shikimic acid and phenethylamine in the effect of scions on rootstocks of *Camellia oleifera*. *Ind. Crops Prod.* **2023**, *203*, 117222. [CrossRef]
21. Liu, Q.; Wang, X.; Zhao, Y.; Xiao, F.; Yang, Y. Transcriptome and physiological analyses reveal new insights into delayed incompatibility formed by interspecific grafting. *Sci. Rep.* **2023**, *13*, 4574. [CrossRef] [PubMed]
22. Castro-Garibay, S.L.; Cruz-Arvizu, O.; Monroy-González, I.; Abarca-Cervantes, A.D.; Cruz-Larios, I.J.; Arguello-Hernández, M. *Pinus cembroides*, and *P. orizabensis* grafts, a viable option for pink pine nut production. *New For.* **2024**, *55*, 1787–1799. [CrossRef]
23. López-Serrano, L.; Canet-Sanchis, G.; Vuletin Selak, G.; Penella, C.; San Bautista, A.; López-Galarza, S.; Calatayud, Á. Pepper rootstock and scion physiological responses under drought stress. *Front. Plant Sci.* **2019**, *10*, 38. [CrossRef] [PubMed]
24. Zeng, J.; Liu, J.; Lian, L.; Xu, A.; Guo, X.; Zhang, L.; Zhang, W.; Hu, D. Effects of scion variety on the phosphorus efficiency of grafted *Camellia oleifera* seedlings. *Forests* **2022**, *13*, 203. [CrossRef]
25. He, W.; Xie, R.; Wang, Y.; Chen, Q.; Wang, H.; Yang, S.; Luo, Y.; Zhang, Y.; Tang, H.; Gmitter, F.G., Jr. Comparative transcriptomic analysis on compatible/incompatible grafts in Citrus. *Hortic. Res.* **2022**, *9*, uhab072. [CrossRef] [PubMed]

26. Wang, Q.; Deng, K.; Ai, J.; Wang, Y.; Wang, Y.; Ren, Y.; Zhang, N. Integrated anatomical and transcriptomic analysis revealed the molecular mechanism of the healing process in homografted and heterografted seedlings of acanthopanax senticosus. *Agronomy* **2023**, *13*, 1527. [CrossRef]
27. Long, W.; Huang, G.; Yao, X.; Lv, L.; Yu, C.; Wang, K. Untargeted metabolism approach reveals difference of varieties of bud and relation among characteristics of grafting seedlings in Camellia oleifera. *Front. Plant Sci.* **2022**, *13*, 1024353. [CrossRef] [PubMed]
28. Yang, J.; Wang, R.; Ren, N.; Zhao, D.-g.; Huang, X.; Zhao, Y. Exogenous application of Eucommia ulmoides β-1, 4-glucanase promotes propagation by increasing the expression of wound healing genes. *Sci. Rep.* **2024**, *14*, 30398. [CrossRef] [PubMed]
29. Li, Y.-X.; Lin, K.-Q.; Wang, A.-R.; Wei, J.; Yan, D.-H.; Zhao, D.-G. Multi-omics analysis of molecular mechanisms driving the grafting-enhanced resistance of tea plants to *Colletotrichum camelliae*. *Front. Plant Sci.* **2025**, *16*, 1750493. [PubMed]

Disclaimer/Publisher's Note: The statements, opinions and data contained in all publications are solely those of the individual author(s) and contributor(s) and not of MDPI and/or the editor(s). MDPI and/or the editor(s) disclaim responsibility for any injury to people or property resulting from any ideas, methods, instructions or products referred to in the content.